Introduction to Chaos: the Damped, Driven, Nonlinear Pendulum

A simple pendulum consists of the usual physicist's massless rod of length l suspended from the usual frictionless pivot, with a bob of mass m attached to its opposite end, and with the usual uniform gravitational acceleration $-g$, as in figure (1). We can write down the kinetic energy T and the potential energy U in terms of the Cartesian coordinates of the bob as

$$\begin{aligned} T &= \frac{1}{2}m\left(\dot{x}^2 + \dot{y}^2\right) \\ U &= -mgy \end{aligned} \tag{1}$$

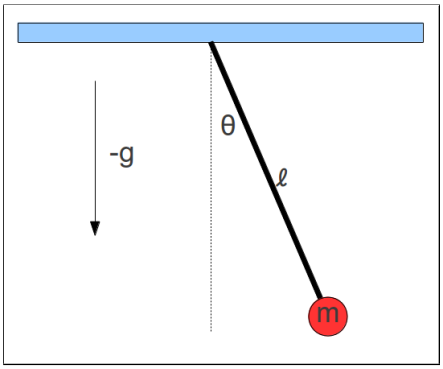

Figure 1: Simple pendulum.

Of course, the bob is not free to move anywhere; it is constrained to follow a trajectory such that the length of the rod does not change:

$$x^2 + y^2 = l^2 \tag{2}$$

This is an example of what is known in mechanics as a *holonomic constraint*. Even though we have two variables to describe the position, they are related by a function so that we have only one degree of freedom in the system. We can thus choose one *generalized coordinate* for the system; in this case, the angle θ which the pendulum makes from the vertical will do nicely; thus, $\theta = 0$ gives the pendulum pointing down. The coordinate transformation is

$$x = l\sin\theta \quad \text{and} \quad y = l\cos\theta \tag{3}$$

and thus we can write the energies as

$$\begin{aligned} T &= \frac{1}{2}m\left(l^2\dot{\theta}^2\cos^2\theta + l^2\dot{\theta}^2\sin^2\theta\right) = \frac{1}{2}ml^2\dot{\theta}^2 \\ U &= -gml\cos\theta \end{aligned} \tag{4}$$

With the energies, we can write the Lagrangian as

$$L = T - U = \frac{1}{2}ml^2\dot{\theta}^2 + gml\cos\theta \tag{5}$$

We can now use the Lagrange equations to derive the equation of motion. The Lagrange equation is

$$\frac{d}{dt}\frac{\partial L}{\partial \dot{q}} - \frac{\partial L}{\partial q} = 0 \tag{6}$$

for generalized coordinates q and generalized momenta $\dot{q}$. We will need the derivatives

$$\begin{aligned} \frac{\partial L}{\partial \theta} &= -gml\sin\theta \\ \frac{\partial L}{\partial \dot{\theta}} &= ml^2\dot{\theta} \\ \frac{d}{dt}\frac{\partial L}{\partial \dot{\theta}} &= ml^2\ddot{\theta} \end{aligned} \tag{7}$$

(remember that the two partial derivatives are with respect to the two *independent* dynamical variables, θ and $\dot{\theta}$; thus, for example, $\partial\dot{\theta}/\partial\theta = 0$.) Putting these in the Lagrange equation, we have the equation of motion

$$\ddot{\theta} = -\omega_0^2\sin\theta \tag{8}$$

where $\omega_0 = \sqrt{g/l}$ is the *natural frequency* of the pendulum. For the rest of this discussion, we will scale the units of time so that $\omega_0 = 1$. The solution exhibits periodic motion, with a period which depends upon the amplitude.[1]

The expression (8) is a second-order ODE, so to compute a numerical solution we re-write it as a system of two first-order ODE's as

$$\begin{aligned} \frac{d\omega}{dt} &= -\sin\theta \\ \frac{d\theta}{dt} &= \omega \end{aligned} \tag{9}$$

The top left panel of Figure (2) shows the solution for the initial conditions $(\theta_0, \omega_0) = (\pi/6, 0)$. For this small amplitude, $\sin\theta \to \theta$ and the solution is very close to simple harmonic motion (the solution to $\ddot{\theta} = -\theta$). Beneath it is a parametric plot of $(\theta(t), \omega(t))$, showing the trajectory of the dynamical system through its phase space. The trajectory is very close to an ellipse. The middle panels of Figure (2) show the solution for larger amplitude, with initial conditions $(0.98\pi, 0)$. The solution no longer looks much like harmonic motion – the pendulum pauses near $|\theta| = \pi$, and the trajectory in the phase plot has taken on a lenticular shape. Finally, in the right panels, the pendulum has been given a strong "kick", with initial conditions $(0, 3)$. The angular velocity stays positive, and the pendulum rotates continuously in an anti-clockwise direction.[2]

We can understand this behavior by considering the total energy of the system, $\frac{1}{2}\omega^2 + (1 - \cos\theta)$, show in Figure (3). The trajectories of the system are along contours of constant energy. The contour which forms an "X", with an energy of 2, is a *separatrix*, a watershed between solutions for which the angular velocity alternates sign (the pendulum swings back and forth) and those for which it remains of constant sign (the pendulum rotates in the same direction).

The Damped Pendulum

This is pretty much all there is to say about the simple pendulum. We can make the problem more interesting by placing the pendulum in a viscous medium. We will assume that the drag force on the pendulum is proportional to its speed (known in fluid mechanics as Stoke's drag), with coefficient γ. Instead of using γ, we will use its reciprocal $Q = 1/\gamma$, the "quality factor" of the oscillator (roughly the number of periods per e-folding in the oscillator's amplitude). Adding this

[1] As an extreme example of how the period depends upon the amplitude, as $\theta \to \pi$ (the pendulum approaches straight up), if $\dot{\theta} \to 0$ the pendulum can take an arbitrarily long time to fall back down. For small amplitudes, however, $\sin\theta \to \theta$ and the system approaches simple harmonic motion in which the period depends only upon the local gravitational acceleration g and the pendulum length l. This made the small-amplitude pendulum the most commonly-used mechanism for measuring time from the 1650's until well into the 20th century. It was calibrated, for most of that interval, by astronomical observations.

[2] A note on coördinate systems. In the coördinate system we have chosen, θ is *periodic* with period 2π. The dynamical equation (8) doesn't know anything about this coördinate system. In a non-periodic coördinate system it is quite happy to provide values for all $\theta \in (-\infty, \infty)$!

If we wish to employ periodic coördinates (say, $\theta \in [-\pi, \pi)$) to display our results, we can enforce this in our solution by a simple expedient: every time we update the value of θ, we apply the rule

$$\theta = \begin{cases} \theta + 2\pi, & \theta < -\pi \\ \theta - 2\pi, & \theta >= \pi \\ \theta, & \text{else} \end{cases} \tag{10}$$

Since $\sin\theta$ and all of its derivatives are continuous for all θ, this will not affect the solution. Alternatively, we can let the solution proceed as it will, and then map the resulting solution onto $[-\pi, \pi)$ before plotting.

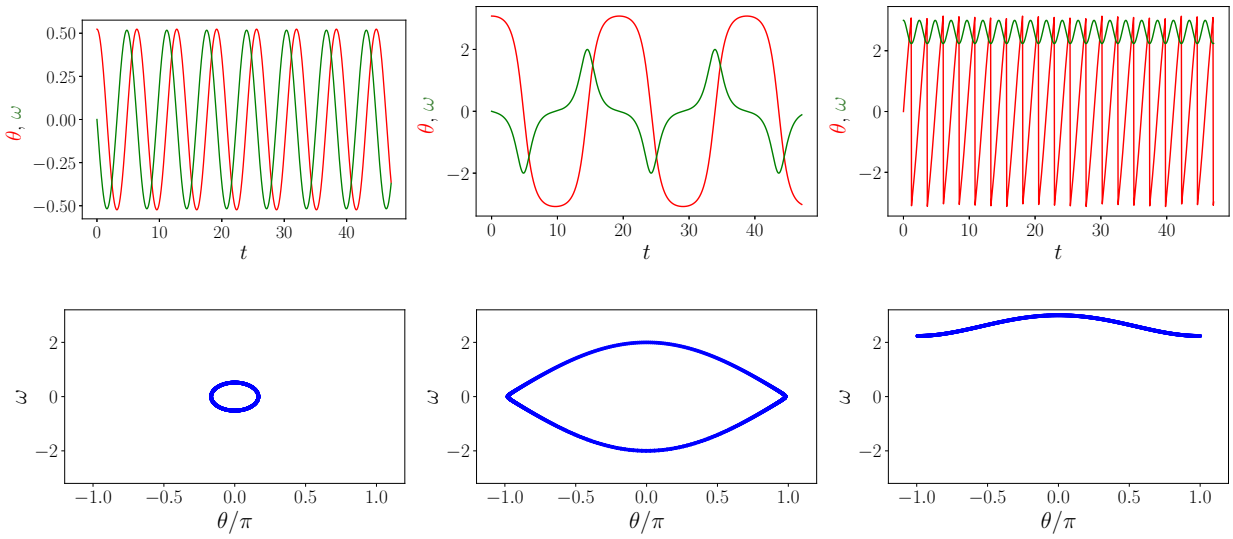

Figure 2: Sample dynamics of a simple pendulum. The top panels show the behavior as a function of time. The bottom panels show the trajectory in phase space. From left to right, the initial conditions are $(\theta_0, \omega_0) = (\pi/6, 0)$, $(0.98\pi, 0)$, and $(0, 3)$.

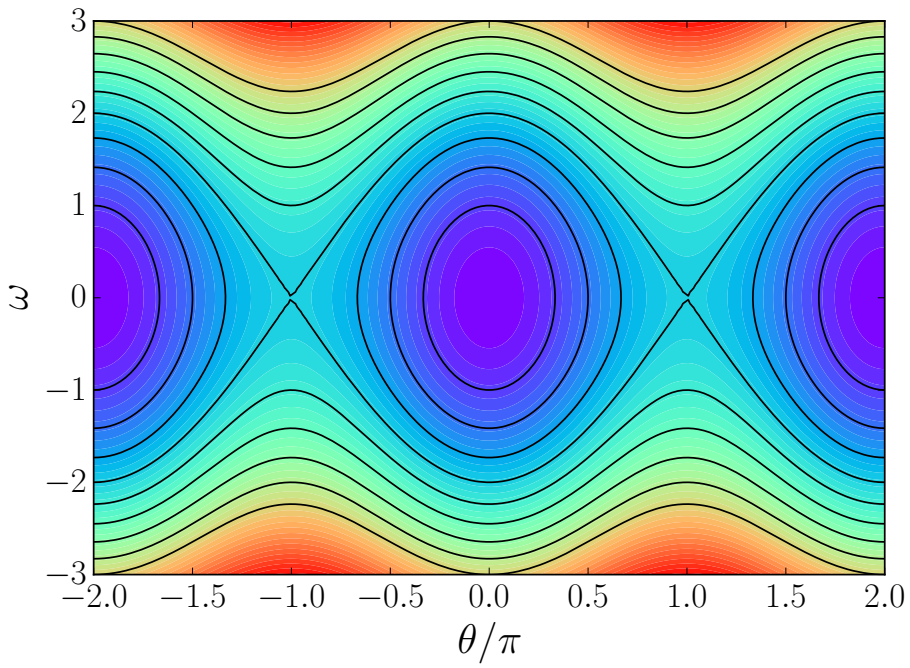

Figure 3: Contour plot of the total energy of the simple pendulum. For a given energy, the motion of the pendulum is constrained to lie on either an elliptical or sinusoidal trajectory (exemplified by the black lines), moving in a clockwise or anti-clockwise direction depending upon the initial conditions.

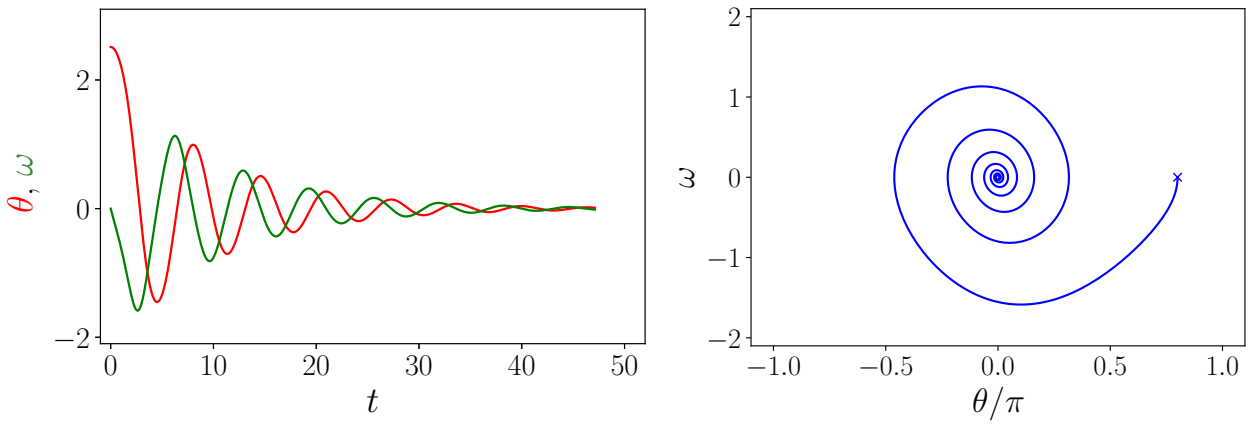

Figure 4: Evolution and phase plot of a damped pendulum. The origin in the phase plot is an attractor for the trajectory which begins at the "x".

drag force to the restoring force, we have the equation of motion of a damped pendulum,

$$\ddot{\theta} = -\sin\theta - \frac{1}{Q}\dot{\theta} \tag{11}$$

The motion of a damped pendulum still isn't very interesting; no matter how we start an oscillation, the amplitude decays and the pendulum eventually stops. The point describing the state of the system in phase space will always approach the origin ($\theta = 0, \omega = 0$) in the phase plot. For small values of damping (large Q) this will be an inward spiral. The origin is thus an *attractor* for the system – the state of the system will be attracted to this location (Figure 4).

The Damped Driven Pendulum

To make matters even more interesting, let us make up the energy lost through damping by adding energy – by driving the system. We can drive the system in many ways. The simplest, commonly seen in an undergraduate physics lab, is to apply a periodic driving torque of amplitude A and frequency ω_D at the pivot:

$$\ddot{\theta} = -\sin\theta - \frac{1}{Q}\dot{\theta} - A\cos\omega_D t \tag{12}$$

where A is measured in units of the length of the rod l. Let's examine its behavior.be asked to write code to simulate this system in the next problem set.)

Clearly, if $A = 0$, the motion is simply a damped oscillation, with the amplitude dying to zero (as in Figure 4). Figure (5) shows the motion of the pendulum with $A = 1.5$ and $Q = 0.5$, for two values of the initial conditions. In these cases we have approximately sinusoidal motion. Initially, the waveform is influenced by the initial conditions, but the "memory" of the starting configuration is damped out in a few cycles and replaced by a steady state, with the phase plot a simple closed curve corresponding to periodic motion, the attractor for these parameters.

We can test to see that the elliptical attractors correspond to periodic motion with period $2\pi/\omega_D$. The top panel of Figure (6) shows the behavior of the system as a function of time, becoming a spiral after an initial transient phase. The phase plot is the projection of this evolution onto the

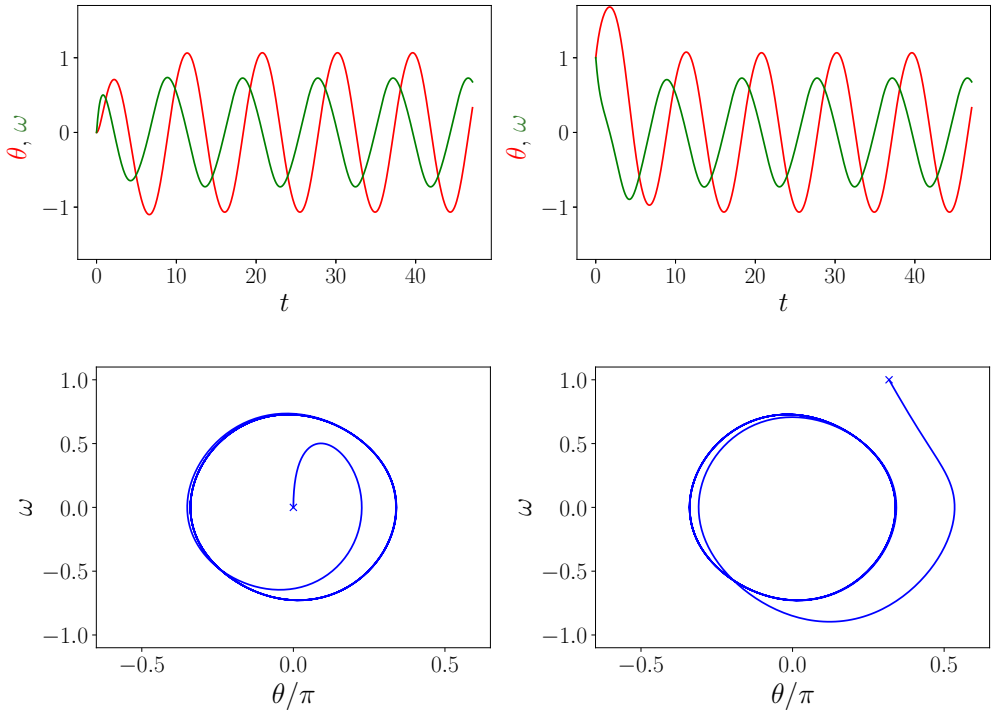

Figure 5: With $A = 1.5$ and $Q = 0.5$, the initial conditions are forgotten in a few cycles, and the system oscillates with the driving frequency ω_D. The plots on the left have initial conditions $\theta_0, \omega_0 = (0, 0)$ while those on the right have initial conditions $(1, 1)$. The system is attracted to the same elliptical trajectory after the initial transient behavior; this is the attractor for this set of parameters.

(θ, ω) phase plane. Now imagine that we cut this spiral at constant intervals of time satisfying

$$\omega_D t_k = \phi + k2\pi, \quad k = 1, 2, \ldots \tag{13}$$

In each cut, the plane of constant time intersects the spiral at a single point. If we then project all of these points down onto the θ-ω plane, we obtain a representation known as a *Poincaré section*. It is stroboscopic view of the phase plot where we plot a point only at the t_k – once per drive period. ϕ is known as the Poincaré phase, and is an arbitrary, but fixed, fraction of the drive period to use as a reference.

When we plot these points on top of our phase plots (Figure 6), we see only a single point. The trajectory returns to the same point every drive period, so we are observing period-1 orbits. We will encounter period-2 and higher orbits shortly.

First, however, let us investigate what happens when we increase Q (decrease the damping). Figure (7) shows the angular velocity at $\theta = 0$ as we increase Q, for the initial conditions $(0, 0)$. The first 50 periods are omitted to avoid seeing the initial transient behavior. As Q increases from $Q = 1.2$, the amplitude of the orbit increases, increasing the angular speed in order to keep the period constant (at the driving period). At $Q \sim 1.245$, however, something new happens.

The top panel of Figure (8) shows the trajectory for $Q = 1.24$. It is much the same as in the previous plots, roughly symmetric about $\theta = 0$. The left panel below it, however, shows that when $Q = 1.3$ the pendulum is now spending more of its time in the region where $\theta < 0$. Why

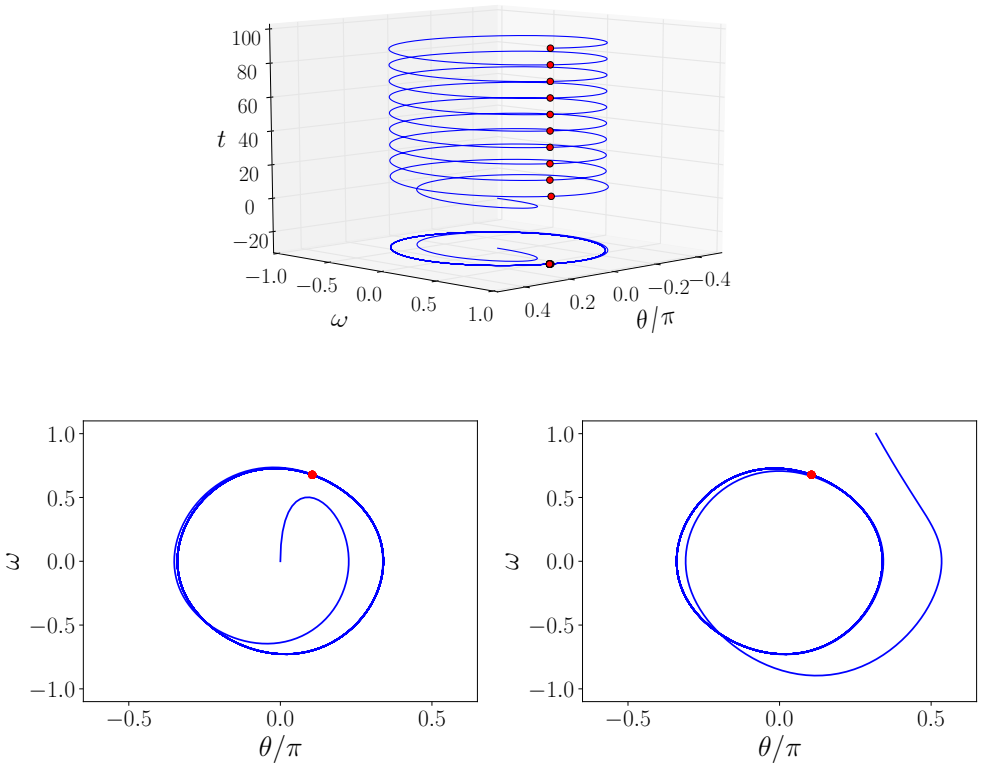

Figure 6: In the top panel, the time evolution of the pendulum is plotted, showing a red point every drive period, along with its projection onto the phase plane. In the bottom two panels, the phase plots are shown with the Poincaré section overplotted. The presence of a single point shows that the attractor exhibits period-1 motion.

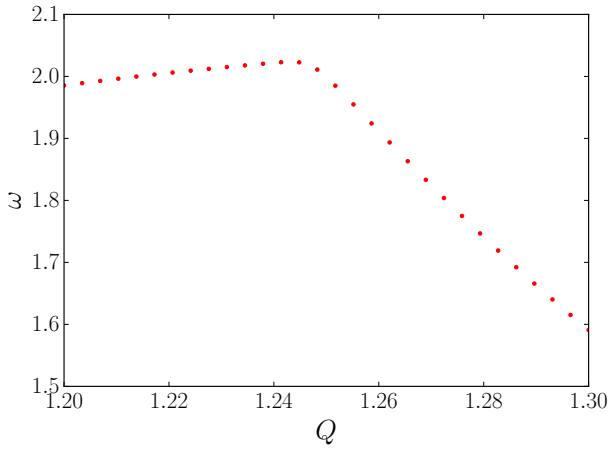

Figure 7: Angular velocity ω at $\theta = 0$ as a function of the Q-factor. Note the break in the trend at $Q \sim 1.245$.

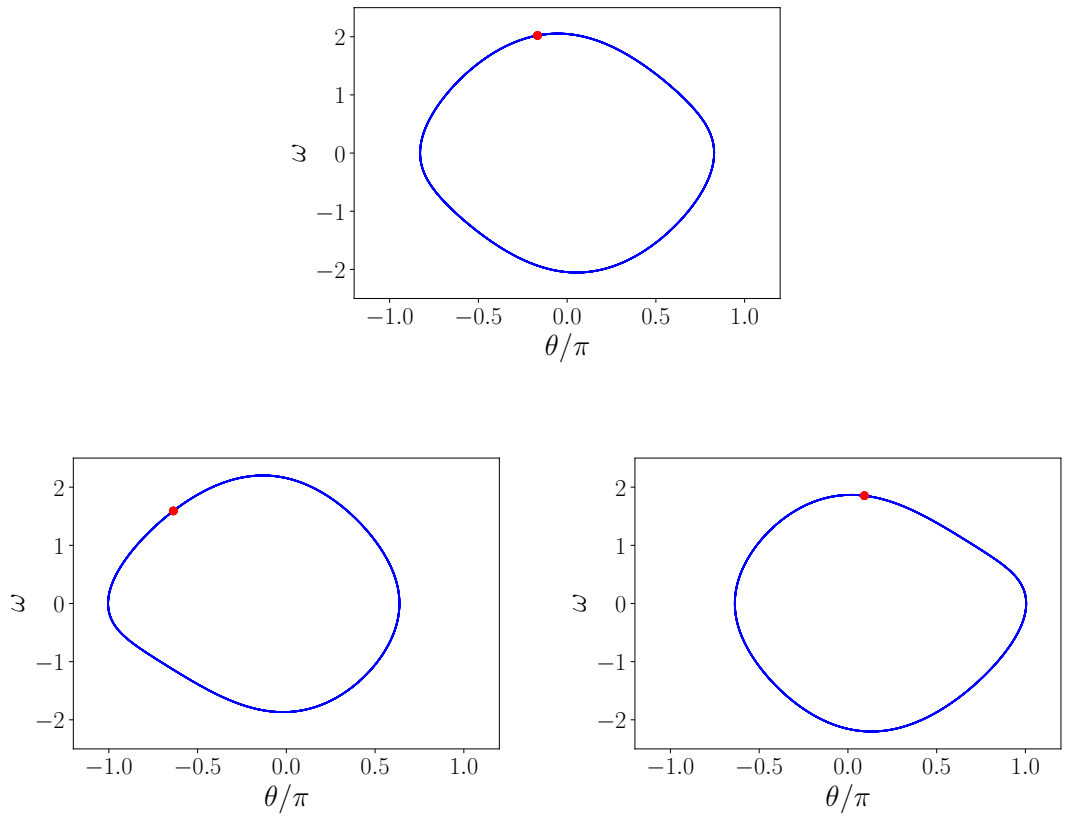

Figure 8: The top panel shows the trajectory of the system for $Q = 1.24$. The left panel on the bottom shows the symmetry-breaking trajectory for $Q = 1.3$ with the initial conditions $(0, 0)$, while the right panel shows the trajectory for the same Q with initial conditions $(0, -3)$.

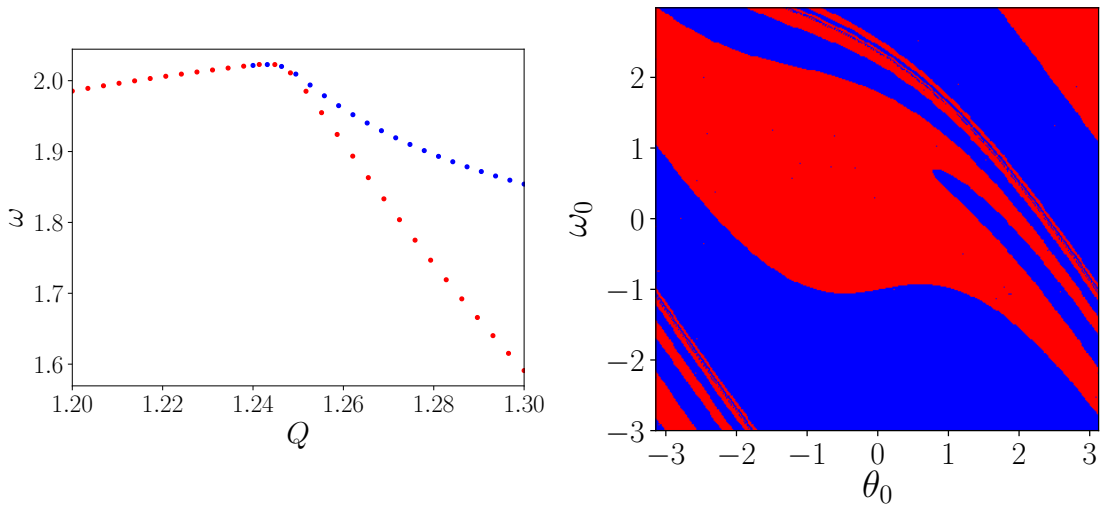

Figure 9: Spontaneous symmetry breaking. The red points in the left panel are the same as those in Figure 7, while the blue points lying above correspond to the initial conditions $(0, -3)$. The right panel shows the division of the plane of initial conditions into basins of attraction to each of the broken symmetry attractors. The red regions correspond to the lower and the blue regions to the upper curves in the left panel.

does this occur? The original equation of motion does not distinguish between the left and the right side of the pendulum – one might say it has a left-right spatial symmetry. This behavior is known as *symmetry breaking* and arises from the nonlinear character of the dynamical system.

Since there is nothing asymmetrical about the dynamical system, we might expect that there is also a solution which favors the region where $\theta > 0$. As can be seen in the right panel of Figure (8), such a solution does exist, the mirror image of the left panel. It arises from changing the initial conditions to $(0, -3)$. If we use both sets of initial conditions to compute the curve shown in Figure (7) we have the left panel of Figure (9). Thus, for values of Q less than the critical value $Q \sim 1.245$, all initial conditions give rise to the same attractor. At the critical value, the attractor *bifurcates* into two asymmetric attractors which are mirror images of each other. Spontaneous symmetry breaking in non-linear dynamical systems plays an important role in many areas of physics; for example, it gives rise to the masses of elementary particles in the Standard Model.

We used two sets of initial conditions to discover symmetry breaking. Which sets of conditions will lead to which attractor? The right panel of Figure (9) shows the θ_0, ω_o plane, colored according to which attractor the solution evolves asymptotically for $Q = 1.3$. When wrapped into a cylinder on the (periodic) θ coordinate, this plot contains only two regions with a single boundary dividing them. This boundary is a *fractal* curve, with complex structure at all scales (the definition of a fractal!). This is a general result – when multiple attractors exist in a dynamical system, the boundary separating them in phase space is a fractal curve. You can think of this boundary as a sort of continental divide on a topographic map; if the system finds itself on either side of the boundary, it is attracted to the corresponding basin.

There in an important caution here for numerical work exploring chaotic systems: the solution at every timestep is the initial condition for the next timestep. Obvious as this may seem, it has profound consequences. Suppose at the end of a timestep we find ourselves in a red region in Figure (9), where the solution is attracted to the left-favoring solution. Now suppose as well that we are very close to the boundary separating the two solutions – since the boundary is a fractal curve, this is a very common occurrence, especially so as the value of Q increases. In this case, a very small numerical error in the solution may place us across the boundary. We now have the initial condition for a solution of the right-favoring trajectory. In a fractal region, an *arbitrarily small* numerical error may cause us to jump from one solution to another.

Even if we were able to solve the ODE analytically, this sort of behavior has important consequences. Because the basins of convergence to a given attractor can be so small, two trajectories whose initial conditions are arbitrarily close may fall into two different basins, leading to entirely different solutions. This extreme sensitivity to initial conditions is one of the hallmarks of a *chaotic system*.

The upper panel in Figure (10) is the continuation of Figure (9) to higher Q. For each value of Q in this diagram we are projecting the Poincaré section onto the ω axis. For each branch (the red and the blue) and for lower values of Q, these are period-1 orbits and we have one point per value of Q for each branch arising from using different initial conditions. Near 1.348, the curves bifurcate; there are now two values of the velocity in the Poincaré section. This corresponds to a transition to the period-2 orbits shown in the lower panels of Figure (10), in which the trajectory travels around the loop twice before retracing itself. The period of the system is now twice the driving period; such a bifurcation is known as a *period doubling*.

The equations of motion for our system are symmetric under the transformation $t \leftarrow t + \tau$, where $\tau = 2\pi/\omega_D$ is the drive period. For low enough values of Q, the behavior of the system reflects this symmetry. As Q is increased beyond ~ 1.348, however, this symmetry is broken. Thus the phenomenon of period-doubling is another manifestation of spontaneous symmetry breaking,

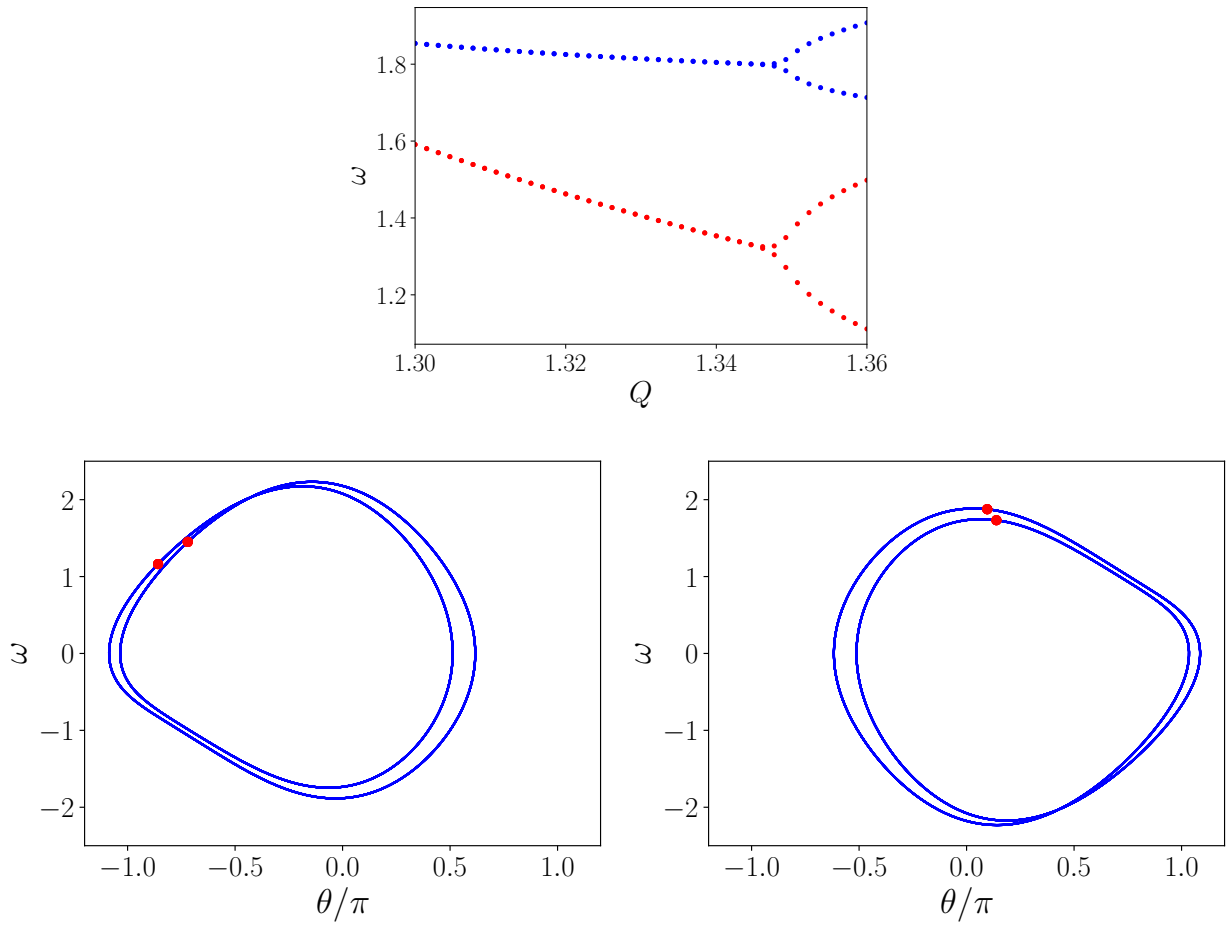

Figure 10: Upper panel: The angular velocity of the Poincaré section for orbits with initial conditions $(0, 0)$ (red) and $(0, -2)$ (blue) as the parameter Q is increased beyond the range explored in Figure 9. Beyond another critical value $Q \sim 1.348$, there are two points in the Poincaré section, signaling a transition to period-2 orbits. This behavior is known as a *period-doubling bifurcation*. Lower panels: Phase plots for $Q = 1.355$. Since the period has doubled, the attractor takes two periods (denoted by the two Poincaré points) before it repeats.

now in time. We see that the spatial symmetry breaking which began at $Q \sim 1.245$ is still present, with temporal symmetry breaking occurring at nearly the same value of Q in both branches.

Figure (11) shows the continuation of the bifurcation plot at the top of Figure (9) to even higher values of Q. After the first period doubling near $Q \sim 1.348$, we see there is a second doubling near $Q \sim 1.370$ when period-4 orbits occur, a third at $Q \sim 1.3755$ leading to period-8, a fourth at $Q \sim 1.3757$ leading to period-16, and so on (see the left two panels of Figure 12). The period-doublings occur at ever-decreasing intervals in Q in an infinite sequence leading to the onset of chaos.

If we let Q_n be the values of Q at the successive doublings, we find the quantity

$$F_n = \frac{Q_{n-1} - Q_{n-2}}{Q_n - Q_{n-1}} \tag{14}$$

the ratio of spacing in Q of successive doublings, rapidly approaches a constant value. This is known as the *Feigenbaum constant*, and has the value $F_\infty = 4.669201....$ Feigenbaum suggested

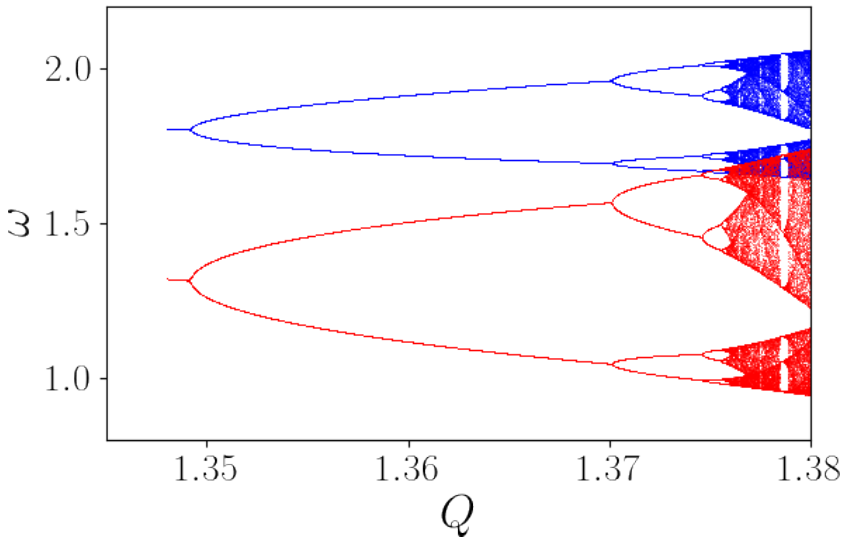

Figure 11: Continuation of the bifurcation plot of Figure 9 to higher values of Q, showing continued period-doubling at increasingly smaller intervals.

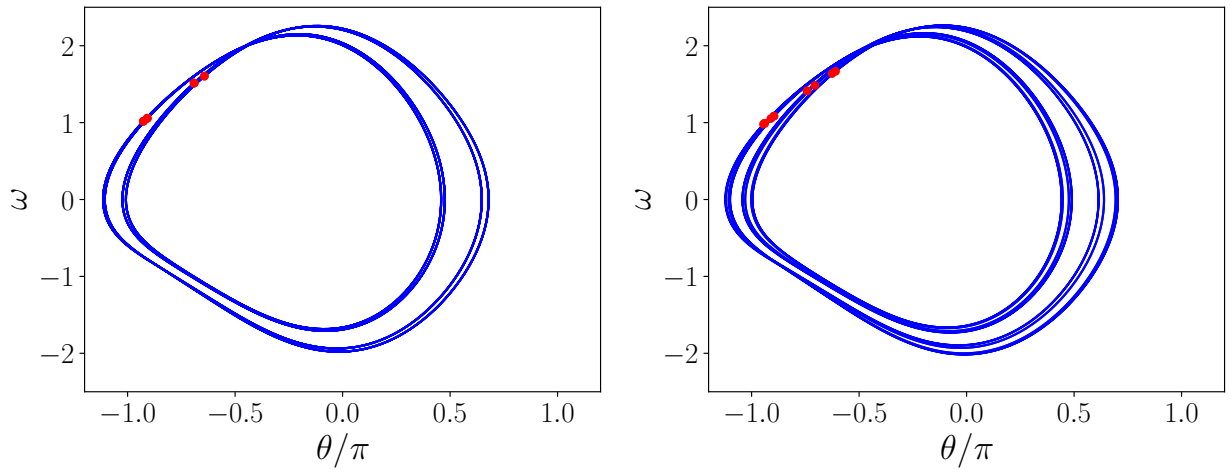

Figure 12: Approach to chaos. In the top panel $Q = 1.371$ with a period-4 attractor; in the middle panel $Q = 1.3753$ and a period-8 attractor. Their Poincaré sections consists of a set of 4 and 8 discrete points, respectively.

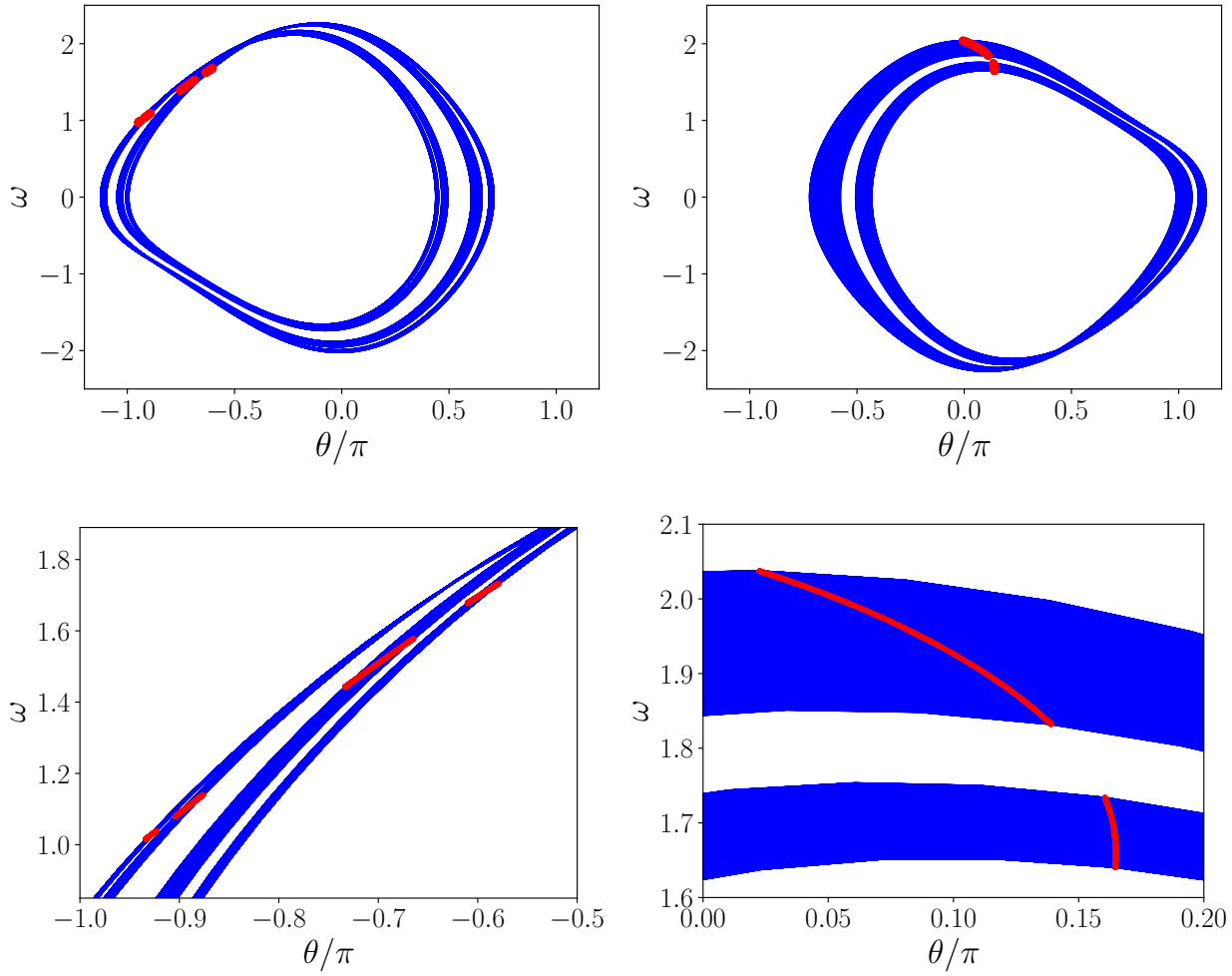

Figure 13: In the left panel, with $Q = 1.376$ and initial conditions $(0, 0)$, the Poincaré section has become four line segments and the attractor now fills regions of phase space, corresponding to trajectories with an infinite winding-number. In the right panel, with $Q = 1.38$ and initial conditions of $(0, -2)$ this evolution becomes even more apparent. The bottom panels are blow-up regions of the panels above.

that this behavior is *universal* in all systems which approach chaotic behavior by period-doubling as a control parameter is increased. If F_n approaches a constant F, we can estimate the value Q_n for the n-th bifurcation as

$$Q_n = Q_1 + (Q_2 - Q_1)\sum_{j=0}^{n-2} F^{-j} \tag{15}$$

The separation between successive period-doubling rapidly decreases (as can be seen from the plot), and Q_n reaches the limiting value

$$Q_\infty = Q_1 + (Q_2 - Q_1)\sum_{j=0}^{\infty} F^{-j} = Q_1 + (Q_2 - Q_1)\frac{F}{F-1} \sim 1.3758 \tag{16}$$

after an infinite number of doublings. An infinite number of doublings corresponds to an attractor, still bounded in the phase plot, but with an infinite period – *i.e.* no period at all! This aperiodic behavior is known as *chaos* and the attractor is a *chaotic attractor*. The phase plot of the attractor thus becomes a solid region within which an infinite number of paths are possible (see the right panel of Figure 13), and the Poincaré section becomes a continuous curve. Such an attractor is known as a *chaotic* attractor since, while the trajectory of the system is still drawn toward it, the trajectory within such an attractor is chaotic.

Figure (14) shows the bifurcation diagram for the damped, driven pendulum extended to $Q = 5$ (with the same other parameters as used above). Note that regions of chaotic dynamics are interspersed with regions where the system returns to apparently periodic motion. This phenomenon is known as *intermittency*, and is another common behavior of periodic systems, perhaps most famously in the energy dissipation of turbulent fluid flow. Understanding this process in detail is beyond the scope of this brief introduction.

A final defining feature of chaotic dynamics is an *exponential sensitivity to initial conditions*. Of course, since every step in the system is the initial condition for its future behavior, this is really a question of the stability of orbits in the system. If we find the system in a certain state, and then perturb the solution, how quickly will the new trajectory approach or diverge from its original trajectory? When a system is chaotic, two trajectories starting from almost identical initial conditions will diverge exponentially in time.

Imagine our pendulum in the state $\mathbf{Z}_0 = (\theta(t_0), \omega(t_0))$, and let the future evolution of the system from this state be $\mathbf{Z}(t)$. Imagine also perturbing the system at t_0, producing the initial state $\mathbf{Z}'(t_0) = \mathbf{Z}(t_0) + \delta\mathbf{Z}_0$, and let the future evolution of this perturbed state be given by $\mathbf{Z}'(t)$. Define the distance between the two orbits as $\delta\mathbf{Z}(t) = \mathbf{Z}(t) - \mathbf{Z}'(t)$. One measure of rate of divergence between the two orbits is the e-folding time of $\delta\mathbf{Z}$, given by

$$|\delta\mathbf{Z}(t)| = |\delta\mathbf{Z}_0|e^{\lambda t} \tag{17}$$

The λ in this expression is known as the *Lyapunov exponent*.[3]

We can examine this sensitivity by integrating the system twice, starting from two nearby sets of initial conditions and measuring the distance between the trajectories as a function of time. In Figure 15 we show the results of such a calculation. To make each plot, the system was evolved long enough to forget its initial transient phase (all were started with initial data $(0, 0)$). Next,

[3]Technically, there are as many Lyapunov exponents as there are dimensions in the phase space; the governing one is the largest – the Largest Lyapunov Exponent, or LLE. In our case, however, both are of similar magnitude, so we will not make that distinction.

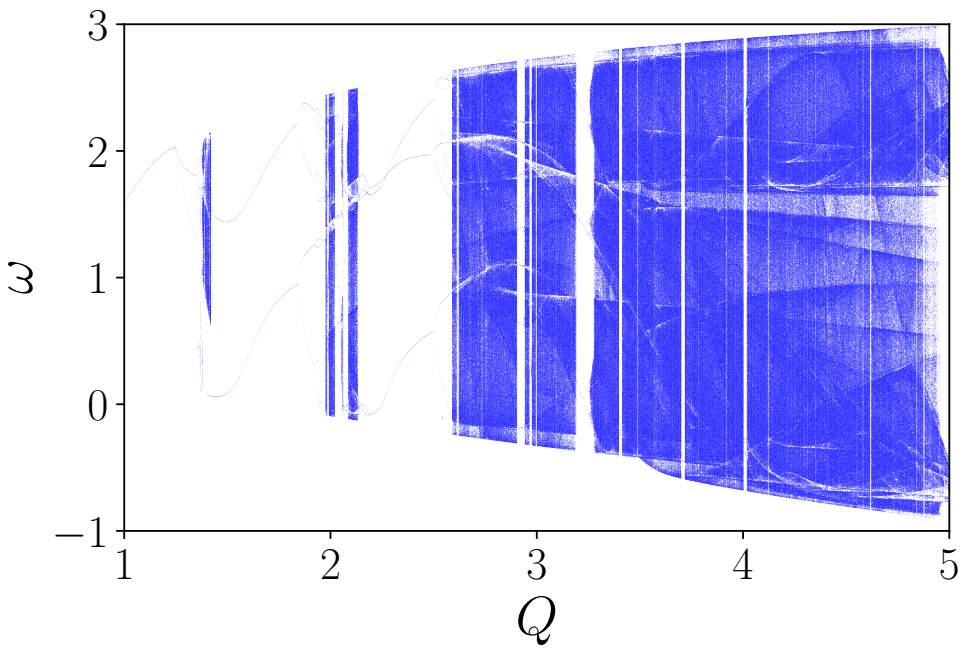

Figure 14: Bifurcation diagram extended to $Q = 5$. The chaotic regime studied above is the narrow band near $Q \sim 1.4$. Above $Q = 1.5$ the system returns to (near) periodic behavior, next becoming chaotic in two distinct regions just above $Q = 2$. These near-periodic regions bounded by chaotic regions are an example of intermittency.

both state variables were perturbed by a small amount (given by the intersection with the left axis in the plots). The two trajectories were then evolved together and the difference between them computed as a function of time.

In the first plot, with $Q = 1.36$, starting with a perturbation of 1e-4, the maximum distance between the trajectories declines exponentially, with $\lambda \sim -2.2$. As we determined above, the phase plot for this system is a simple closed curve; no matter what the initial conditions, all orbits of the system in the phase plot are attracted to it. In the second plot, run with $Q = 1.377$, the system is into the chaotic regime, and the trajectories diverge with $\lambda \sim 0.28$. The last plot, with $Q = 1.4$, is well into the chaotic regime and the trajectories diverge with $\lambda \sim 0.83$. Note that, as measured, the divergence cannot continue to increase forever, since $\Delta\theta$ can never grow beyond 2π, but it is clear that after a short time, the trajectories become completely different in spite of the almost identical initial conditions.

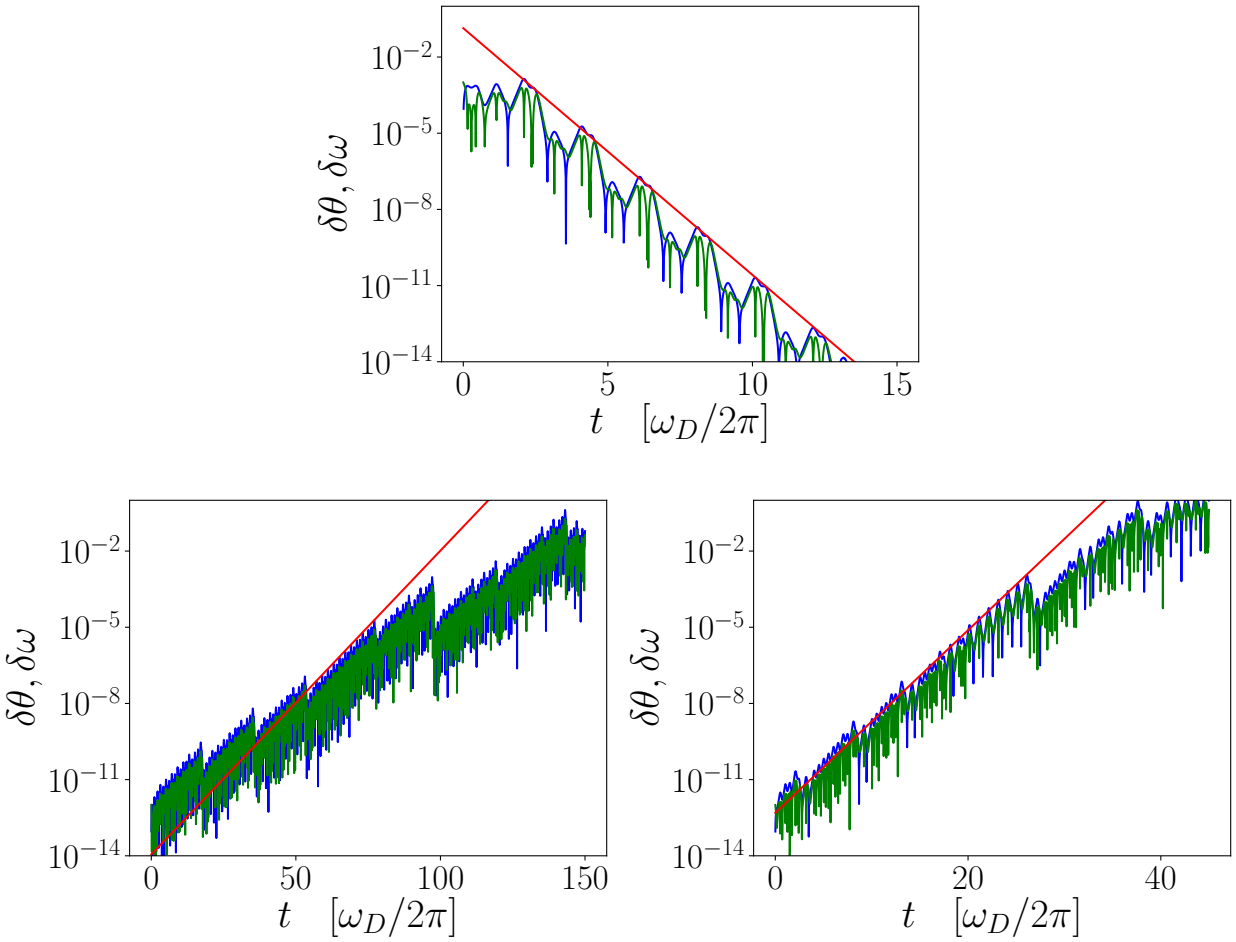

Figure 15: Stability of trajectories in phase space. Plotted is the difference between the original trajectory and a perturbed trajectory *vs.* time in drive periods. $\delta\theta$ is shown in blue and $\delta\omega$ in green. The slope of the red lines (crude fits!) give the Lyapunov exponents for each. Upper panel: $Q = 1.36$ and the trajectory is drawn to the attractor. Left panel: $Q = 1.377$ near the onset of chaos. Right panel: $Q = 1.4$, a strongly chaotic trajectory.